



The mitochondrial carrier homolog 2 is involved in down-regulation of influenza A virus replication

Pınar Ulupınar¹ · Elif Çağlayan² · Erkan Rayaman³ · Kyosuke Nagata⁴ · Kadir Turan³

Received: 7 December 2023 / Accepted: 25 April 2024
© The Author(s), under exclusive licence to Springer Nature B.V. 2024

Abstract

Background The mitochondrial carrier homolog 2 (MTCH2) is a mitochondrial outer membrane protein regulating mitochondrial metabolism and functions in lipid homeostasis and apoptosis. Experimental data on the interaction of MTCH2 with viral proteins in virus-infected cells are very limited. Here, the interaction of MTCH2 with PA subunit of influenza A virus RdRp and its effects on viral replication was investigated.

Methods The human MTCH2 protein was identified as the influenza A virus PA-related cellular factor with the Y2H assay. The interaction between GST.MTCH2 and PA protein co-expressed in transfected HEK293 cells was evaluated by GST-pull down. The effect of MTCH2 on virus replication was determined by quantification of viral transcript and/or viral proteins in the cells transfected with MTCH2-encoding plasmid or MTCH2-siRNA. An interaction model of MTCH2 and PA was predicted with protein modeling/docking algorithms.

Results It was observed that PA and GST.MTCH2 proteins expressed in HEK293 cells were co-precipitated by glutathione-agarose beads. The influenza A virus replication was stimulated in HeLa cells whose MTCH2 expression was suppressed with specific siRNA, whereas the increase of MTCH2 in transiently transfected HEK293 cells inhibited viral RdRp activity. The results of a Y2H assay and protein-protein docking analysis suggested that the amino terminal part of the viral PA (nPA) can bind to the cytoplasmic domain comprising amino acid residues 253 to 282 of the MTCH2.

Conclusion It is suggested that the host mitochondrial MTCH2 protein is probably involved in the interaction with the viral polymerase protein PA to cause negative regulatory effect on influenza A virus replication in infected cells.

Keywords MTCH2 · Influenza PA protein · Viral RdRp · Yeast two hybrid · Protein–protein docking

Introduction

The human mitochondrial carrier homolog 2 (MTCH2) protein is closely related to the mitochondrial carrier (MC) protein family [1, 2]. The members of the MC protein family are mostly located in the inner mitochondrial membrane; they play a role in many important metabolic pathways such as oxidative phosphorylation, fatty acid oxidation, the citric acid cycle, gluconeogenesis, lipogenesis, and ketone body production and utilization [3]. The MTCH2, structurally similar to MC proteins, is functionally not characterized very well. In some studies, the MTCH2 protein has been associated with programmed cell death (apoptosis) [4, 5]. It has been suggested that MTCH2 acts as a receptor for BID in mitochondria and plays a critical role in Fas-mediated apoptosis [6]. On the other hand, it is associated with Alzheimer's, obesity, and diabetes due to its effects on mitochondrial metabolism [7, 8]. The reports showing the

✉ Kadir Turan
kadirturan@marmara.edu.tr

¹ Institute of Health Sciences, Marmara University, Istanbul, Turkey

² University of Health Sciences, Kartal Koşuyolu High Speciality Educational and Research Hospital, Istanbul, Turkey

³ Department of Basic Pharmaceutical Sciences, Faculty of Pharmacy, Marmara University, Istanbul, Turkey

⁴ Department of Infection Biology, Graduate School of Comprehensive Human Sciences, University of Tsukuba, Tsukuba, Japan

interaction of the MTCH2 protein with viral proteins are limited [9]. However, the relationship of the MTCH2 protein with apoptosis may be important in terms of its direct or indirect effect on the virus replication. Many viruses have positive or negative controls on apoptosis pathways in order to replicate effectively in the host cell [10, 11]. It is known that influenza A viruses affect cellular processes such as host cell proliferation, protein synthesis, autophagy, and apoptosis through various proteins encoded from their genome [12, 13]. In this study, the interaction of the PA protein, which is a subunit of the influenza A virus RNA polymerase, with human MTCH2 was demonstrated by a yeast two-hybrid (Y2H) assay.

Influenza A viruses belong to the *Orthomyxoviridae* family and have a negative polarity single-stranded RNA genome consisting of eight segments [14]. Replication and transcription of the viral RNAs in infected cells are catalyzed by the RNA-dependent RNA polymerase (RdRp) composed of polymerase basic protein 2 (PB2), polymerase basic protein 1 (PB1), and polymerase acidic protein (PA). These proteins are carried as bound on the helical hairpin of viral RNAs resulting from base pairing between the conserved semi-complementary 5'- and 3'-ends [14, 15].

The RdRp synthesizes viral RNA through the cRNA intermediate without a primer, while performing the viral mRNA transcription in a primer-dependent manner. A short-capped oligomer derived from host nascent pre-mRNA is utilized to prime transcription of viral mRNAs [16, 17]. Both PB2 and PA subunits are involved in this process; PB2 binds to a 5'-cap of nascent host mRNA, and PA cleaves the 10–15 nucleotide with endonuclease activity [18]. In many studies, it has been reported that the influenza PA protein affects the viral replication process by interfering with some cellular events in addition to the basic functions in viral replication/transcription. It has been suggested that the PA protein plays a role in the inhibition of the host type I interferon signaling pathway [12]. Some point mutations in this protein affect the virulence of the virus [19] and have immunomodulatory effects [20]. In this respect, the PA protein can be considered as a multifunctional protein.

In this study, it was revealed that the carboxyl-terminal region of the MTCH2 protein interacts with the viral PA protein, and the influenza A virus replication is up-regulated in MTCH2 gene knockdown cells, whereas the increase of MTCH2 expression in the cell inhibits the viral RdRp enzyme activity. Considering the Y2H assay data and viral RdRP complex structure, possible PA and MTCH2 interaction models were predicted using bioinformatics database, and protein modeling/protein-protein docking tools. Although the inhibition mechanism resulting from the interaction of MTCH2 and PA proteins on viral replication is not

fully understood, it is believed that these two proteins cause this effect through an apoptotic pathway.

Materials and methods

Yeast cells

A Y2H screening assay was performed with the *Saccharomyces cerevisiae* strain PJ69-4 A (*MATa trp1-901 leu2-3,112 ura3-52 his3-200 gal4(deletion) gal80(deletion) LYS2::GAL1-HIS3 GAL2-ADE2 met2::GAL7-lacZ*) [21]. This strain contains the TRP and LEU2 transformation markers and the ADE2, HIS3 reporter genes, as well as the lacZ from *Escherichia coli* encoding β -galactosidase controlled by GAL4 response elements. The yeast was grown in a YPD (1% - w/v yeast extract, 2% - w/v peptone, 2% - w/v dextrose) and/or YPAD (YPD + 100 mg/L of adenine sulfate) medium at 30 °C, 180 rpm constant shaking. For agar plates, 2% - w/v agar was added to the media.

Mammalian cells

The HEK293 (human embryonic kidney cells) and HeLa (cervical cancer cells) cell lines were used in transient protein expression and/or viral infection. The cells were grown in low glucose (1 g/L) Dulbecco's Modified Eagle's Medium (DMEM) (Gibco #31600083) supplemented with 10% fetal bovine serum (Gibco #10270106), 2 mM glutamine, penicillin (100 U/mL), and streptomycin (100 μ g/mL) and incubated in an incubator at 37 °C under 5% CO₂ and 95% air humidity.

Bacterial strains

The *Escherichia coli* DH5 α , Mach1, and Top10 strains were used during the cloning of genes and amplification of plasmids. The bacteria were cultured in Luria-Bertani (LB) broth (1% - w/v Tryptone, 0.5% - w/v Yeast Extract, NaCl 1% - w/v). For solid LB medium (LBA), 1.5% - w/v agar was added.

Viruses

Human influenza A/WSN/33-H1N1 (WSN) and avian influenza A/duck/Pennsylvania-H5N2 (DkPen) viruses were used in infection experiments to detect the effects of host proteins on viral replication and their interactions with the viral PA protein. The viruses were obtained from the Department of Infection Biology, Faculty of Medicine, Tsukuba University (Japan).

Plasmids and construction of expression vectors

The plasmids pGBD-C1 [21] and pCHA [22] were used to construct vectors expressing bait protein in yeast and human MTCH2 in mammalian cells, respectively. Influenza A virus minireplicon plasmids were constructed as previously described [23, 24].

In the Y2H screening assays, a bait protein (nPA-GBD) consisting of the amino-terminal half of the influenza A DkPen PA (nPA: 1-359, amino acids) bound to the amino-terminal end of the yeast GAL4 transcription factor binding domain was used. The plasmid vector encoding this bait protein was obtained by cloning the viral PA cDNA into the pGBD-C1 plasmid. The pGBD-C1 plasmid DNA was linearized just before the start codon of the GAL4-BD coding sequence by inverse PCR using the GAL4-For and GBDvec-Rev primers (Table 1). The PCR was performed using the high fidelity KOD DNA polymerase enzyme (Toyobo #KOD-201) in the following cycling conditions: initial denaturation for 3 min at 97 °C, 32 cycles of 15 s at 97 °C, 20 s at 54 °C, 5 min at 68 °C, and a final extension

for 15 min at 68 °C. The PCR product was purified with an agarose gel extraction kit (Invitrogen #K210012). The viral nPA cDNA was amplified with KOD DNA polymerase using phosphorylated PA/DkPen-For and nPA/DkPen-GGSG-Rev primers and pCAGGS-PA(D) [23] plasmid DNA as a template. The primers were phosphorylated with T4 polynucleotide kinase (NEB #M0201). The PCR cycling condition was an initial denaturation at 97 °C for 3 min, 32 cycles of 15 s at 97 °C, 15 s at 53 °C, 45 s at 68 °C, and a final extension at 68 °C for 10 min. The PCR product was purified with an agarose gel extraction kit. Linearized pGBD-C1 plasmid DNA and viral nPA cDNA was ligated with T4 DNA ligase (TaKaRa #2011), and the resultant plasmid was named pGBD-nPA.GAL4.

In order to increase the MTCH2 protein level in transiently transfected cells, the MTCH2 gene was cloned in a pCHA plasmid under the control of a chicken β actin promoter. MTCH2 v.3 (NCBI: NP_001304162.1) cDNA was amplified by PCR using MTCH2-specific phosphorylated MTCH2-For/MTCH2-Rev primers (Table 1) and the HeLa cDNA library as a template and purified with an agarose gel extraction kit. pCHA plasmid DNA was digested with the EcoRV (NEB #R0195) enzyme and then dephosphorylated with Shrimp Alkaline Phosphatase (SAP) (ThermoFisher #78390). Digested pCHA plasmid DNA and MTCH2 cDNA were ligated with T4 DNA ligase, and the resulting plasmid was named pCHA-MTCH2.

For the GST pull down assay, MTCH2 v.3 cDNA was cloned downstream of the GST ORF in the pCAGGS-GSTnls plasmid vector [25]. The linearized pCAGGS-GSTnls DNA was created with inverse PCR using pCA-Vec-For and GST(GGSG)-Rev primers (Table 1). The MTCH2 v.3 ORF prepared as mentioned above was ligated with linear pCGAAS-GSTnls. The resulting plasmid vector was named pCAGGS-GST-MTCH2. The plasmid vector encoding the PA protein with a C-terminal double Flag epitope (PA.FF) was derived from the pCAGGS-PA(W) plasmid [23]. The 3'-terminal part of the PA gene was amplified using KOD DNA polymerase and the pCAGGS-PA(W) template with the PA(W)-1485-For and PA(W)-FF-Rev primers (Table 1). The PCR product was digested with AflII (NEB #R0520) and BglII (NEB #R0144) enzymes and purified with an agarose gel extraction kit. The pCAGGS-PA(W) plasmid DNA was cut with AflII and BglII, dephosphorylated with SAP, and the large plasmid fragment was purified. The PCR product carrying the FF sequence was ligated with the plasmid DNA and resulting plasmid was named pCAGGS-PA.F. pCAGGS-Myc.PA, which encodes PA with the Myc epitope at the N-terminus, was kindly provided by Dr. Fumitaka Momose (Kitasato University, Japan).

The small scale plasmid DNAs were prepared with the alkaline-lysis method [26], and gene sequences were

Table 1 Oligonucleotide primers used in different stages of the study

Name	Sequence
GAL4-For	5'-ATGAAGCTACTGTCTTCTATC G-3'
GBDvec-Rev	5'-CTTTCAGGAGGCTTGCTTCA AG-3'
PA/DkPen-For	5'-ATGGAAGACTTTGTGCGACA ATGC-3'
nPA/DkPen-GGSG-Rev	5'-tccagatcctccGTCTTTT- GTCTTTGGGATCTTC-3'
MTCH2-For	5'-ATCATGGTACAGTTCATTGGC AG-3'
MTCH2-Rev	5'-ATTCAAATTAACATTTTCAGG TCAC-3'
GAD424-For	5'-AATACCACTACAATGGATGAT GT-3'
GAD424-Rev	5'-CCAAGATTGAACTTAGAGG AGT-3'
GAD424sq-For	5'-CGATGATGAAGATACCCAC-3'
ACTB-QF	5'-CCACACCTTCTACAATGAGC-3'
ACTB-QR	5'-TCATGAGGTAGTCAGTCAGG-3'
Seg8/WSN-QF	5'-TGATGCCCCATTCCCTGA-3'
Seg8/WSN-QR	5'-TACAGAGGCCATGGTCATTT-3'
Seg8/DkPen-QF	5'-TCATCGGTGGACTTGAATGG-3'
Seg8/DkPen-QR	5'-TCTGACTCAACTCTTCTCGC-3'
pCA-Vec-For	5'-AGATCTTTTCCCTCTGCCAA AATTATG-3'
GST(GGSG)-Rev	5'-tccagatcctccCAGATCCGATTTG- GAGGATGGTC-3'
PA(W)-1485-For	5'-GTAGAATAAGGAGGAAG G-3'
PA(W)-FF-Rev	5'-tttAGATCTTTCATTATCAT- CATCTTTATAATCTTTATCA TCATCTTTATAATCTCTCAATGCAT GTGTGAGGAAG-3'

confirmed by Sanger sequencing. Then, midi-scale plasmid DNA isolations and purifications were performed using a Plasmid Midi Kit (Qiagen #12145).

DNA library construction and amplification for Y2H screening

The cDNA library for Y2H screening was obtained by cloning the cDNAs prepared from HeLa cells into the pGAD424 plasmid vector. A cDNA synthesis kit (TaKaRa #6120) was used for the preparation of the cDNA by following the kit manufacturer's guidance. The cDNA was cloned into the EcoRI site in the pGAD424 plasmid. After first step amplification in competent *E. coli* DH5 α with high transformation efficiency (competent cell kit: Toyobo #DNA-903), the cDNA library was transformed into electrocompetent *E. coli* Top10 cells (Invitrogen #C404052) by the electroporation method. For this, 2 μ l (250 ng) cDNA library (cloned in pGAD424) was added to 50 μ l of electrocompetent cell suspension. A single pulse (2000 V-5 mSec) for a 100 μ l electroporation cuvette (Eppendorf AG #94) was applied with an electroporation apparatus (Electroporator 2510, Eppendorf, Germany), and 750 μ l of LB broth was immediately added to the cells. The cell suspension was diluted to 10 ml with LB broth and spread on 150 cm LB agar plates (+ amp) (400 μ l/plate) and incubated at 35 °C for 48 h. The bacterial colonies on each LB plate were collected in 10 ml LB broth with a glass baguette (approximately 200 ml). Plasmid DNA was isolated from the cells by the alkaline-lysis method [26]. 10 μ l of RNase A (10 mg/ml) was added to a one ml DNA sample in TE buffer and incubated for 15 min at room temperature. Then, the sample was mixed with 4 volumes of PEG (20% - w/v)/NaCl (1.25 M) solution, incubated on ice for 60 min, and centrifuged at 15,000 rpm at 4 °C for 25 min. The DNA precipitate was washed with cold 70% - v/v EtOH, dried, dissolved in TE, and checked with agarose gel electrophoresis. To check for the different insert cDNA content of the amplified cDNA library, a small amount of plasmid DNA was transformed into chemically competent *E. coli* Mach1 cells. Twenty randomly selected colonies grown on the LB plate (+ amp) were examined by colony-PCR for inserting DNA using primer pair GAD4-F and GAD4-R (Table 1) targeting the insert borders. Agarose gel electrophoresis showed that, on average, 80% of the colonies carried cDNA of varying sizes (data not shown). The quality-checked cDNA library was used for the transformation of yeast cells for Y2H screening.

Transformation of yeast cells and selection of positive colonies

Y2H screening was carried out with *S. cerevisiae* strain PJ69-4 A. The yeast cells were transformed in two steps. In the first step, the cells were transformed with the plasmid DNA (pnPA-GBD) encoding nPA-GAL4.BD bait. Transformation was performed by the lithium acetate/SS carrier DNA/polyethylene glycol (LiAc/SS-DNA/PEG) method [27]. The single transformant colony encoding the bait protein was selected on a synthetic drop-out (SD) plate (without TRP). A culture was prepared from the yeast colonies harboring the bait plasmid, and the cells were transformed with the Y2H-cDNA library using the LiAc/SS-DNA/PEG method. The positive transformants were selected by growing on SD plates (without trp/leu/his/ade) supplemented with 2 mM 1,2,4 triazole (3-AT) for 3–4 days at 30 °C. After the first step selection, the reporter β -galactosidase activities of the yeast colonies were determined. The yeast colonies were grown in 5 ml SD (without trp/leu/his/ade) at 30 °C with shaking at 200 rpm for 16–20 h, 250 μ l of saturated yeast cultures were centrifuged at 3500 rpm for 5 min, and cell precipitates were suspended in 300 μ l of Buffer Z (100 mM sodium phosphate buffer, 10 mM KCl, 1 mM MgSO₄). The cell suspensions were subjected to freeze-thaw cycles (5 times) in liquid nitrogen and in a water bath (at 37 °C). Then, 1 μ l of 2-mercaptoethanol and 60 μ l of ONPG (4 mg/ml) substrate solution were added into each sample and incubated for 1–2 h at 30 °C. The reaction was stopped by adding 300 μ l of 0.5 M Na₂CO₃ on the samples. The cellular debris were removed by centrifugation at 15,000 rpm for 5 min, and the absorbance of the supernatants at 420 nm was measured. Relative β -galactosidase activities of the samples compared to the control cells (harboring the bait plasmid) were determined.

Identification of the candidate gene

Plasmid DNA was isolated from the yeast colonies grown on SD plates (without trp/leu/his/ade) having high relative β -galactosidase activity by using a yeast plasmid DNA isolation kit (Bio Basic #BS459). The candidate cDNAs were amplified with PCR using the GAD424-F/GAD424-R primer (Table 1) pairs bound to their borders and the plasmids as template and then purified. The sequences of the purified cDNAs were identified by Sanger sequencing with GAD424sq-For primer (Table 1) followed by BLAST analysis. In this study, we focused on the MTCH2 protein, which is one of the candidate interactor proteins of viral PA, because of triggering of apoptosis in host cells under viral infection conditions.

Plasmid DNA transfection

HEK293 or HeLa cells were seeded in 12-well ($1\text{--}2 \times 10^5$ cells/well) or 24-well (5×10^4 cells/well) plates and incubated at 37 °C for 24 h. The cells in each well were transfected with 0.3–1 µg of plasmid DNA. For this, plasmid DNAs were diluted in OPTI-MEM (Gibco #31985047) at a concentration of 15 ng/µl. A transfection reagent (GeneJuice, Novagen #70967) was diluted 1/22 in OPTI-MEM and mixed with an equal volume of diluted DNA samples (average ratio: 3 µl reagent for 1 µg DNA). For complex formation, the mixture was left for 5 minutes at room temperature and added to culture media. After 40–48 h of incubation under standard culture conditions, the cells were examined with Western blotting, immunofluorescence staining, or minireplicon assay.

siRNA transfection

The MTCH2 gene in HeLa cells was knocked down using MTCH2 gene-specific siRNA. 20–30 pMol of MTCH2-siRNA (Life Technologies #1299001/HSS119218) was diluted in 125 µl of OPTI-MEM. Three µl of RNAi-max (Invitrogen #13778075) diluted in an equal volume of OPTI-MEM was mixed with diluted siRNA and incubated at room temperature for 5 min. For the control, a negative control siRNA (Santa Cruz #sc-37007) was similarly prepared.

HeLa cells grown in DMEM were suspended with Trypsin (0.1%) - EDTA (0.05%) solution and precipitated by centrifugation at 1000 rpm for 5 minutes. The cells were re-suspended in OPTI-MEM, counted with a hemocytometer, and adjusted to 5×10^5 cells/ml cell density. siRNA/RNAi-max samples were added to 0.5 ml cell suspension (2.5×10^5 cells) in 1.5 ml tubes and mixed at moderate speed in a vertical tube mixer at 37 °C for 30 min. The samples were then transferred to 6-well plates containing 2 ml of DMEM and incubated for 48 h under standard culture conditions. After incubation, the cells were suspended with Trypsin-EDTA and counted with a hemocytometer. RNA extraction was performed for the quantitation of MTCH2 transcripts from a portion of cells. A portion of siRNA-transfected and non-transfected cells (as a control) were seeded in 12-well plates (5×10^5 cells/well), and 24 h after incubation, the cells were infected with a MOI of 0.2 influenza A (WSN) or (DkPen) viruses. The RNA extraction was performed from some of the infected samples for quantitation of viral RNAs at the 8th hour of infection. After reverse transcription, the viral RNA, viral cRNA/mRNA, and ACTB transcript levels were analyzed by quantitative PCR (qPCR). Some infected samples were harvested at 12 h post infection, and viral and cellular β -Actin proteins were analyzed with Western blotting.

Western blot analysis

Expression of the viral and cellular proteins in the cells transfected and/or infected with influenza A viruses was detected with immunoblotting. The cells were lysed in SDS-sample buffer, the proteins were separated by 10% SDS-PAGE, and then transferred to a PVDF membrane. The membranes were blocked with 5% non-fat milk (in TBS-T) and probed with primary antibodies diluted in blocking solution. After washing with Tris-Buffered Saline (TBS: 50 mM Tris pH.8, 138 mM NaCl, 2.7 mM KCl), and TBS-T (TBS + 0.1% Triton X-100), the membranes were treated with goat anti-mouse IgG-HRP (Invitrogen #31420) or anti-rabbit IgG-HRP (Invitrogen #31423) secondary antibodies. The proteins were visualized with ECL detection kit (GE Healthcare #RPN2235) using a gel imaging system (DNR Bio-Imaging system, Israel).

Co-expression of MTCH2 and PA proteins in the cells, and GST pull-down assay

HEK293 cells were seeded in 10 cm petri dishes (3×10^6 cells/petri) and incubated overnight under standard culture conditions. The cells were transfected with a mixture of pCAGGS-GST-MTCH2 (4.5 µg) and either pCAGGS-PA.FF or pCAGGS-Myc.PA (3 µg) using PEI as described previously [13]. To monitor transfection efficiency, pEGFP-N1 reporter plasmid DNA (Clontech) (0.1 µg) was added to the DNA mixture. Forty-eight hours after transfection, the media were removed and the monolayers were washed with PBS, and then incubated with 2 mM dithiobis (succinimidylpropionate) (DSP) at 4 °C for 1 h. After that, glycine was added to the samples to achieve a final concentration of 100 mM, and the DSP-glycine solution was removed. The cells were collected in 0.75 ml buffer A (50 mM Tris, pH.8, 150 mM NaCl, 1 mM EDTA, 0.1% NP40) using a scraper, lysed by freeze and thaw cycles (liquid nitrogen : 37 °C) followed by passing through 27G needle. The lysates were centrifuged at 14,000 rpm for 10 min at 4 °C, and the supernatant was used for analysis of protein expression and GST pull-down. A 100 µl of a 50% slurry of glutathione-agarose beads (Thermo Scientific #16100) equilibrated with wash buffer (50 mM Tris, pH.8, 150 mM NaCl) was added to the 500 µl of supernatant and mixed for 4 h at 4–6 °C. The samples were centrifuged at 2500 rpm for 2 min and the supernatant was removed. The beads were washed twice with wash buffer by mixing for 5 min. The precipitates were suspended in 100 µl x2 SDS-PAGE sample buffer and the proteins were denatured at 95–100 °C for 5 min. The proteins underwent analysis through SDS-PAGE/Western blot, as described in Sect. [Western blot analysis](#) using rabbit polyclonal anti-GST antibody (Abcam #ab9085) (for GST).

MTCH2), mouse monoclonal anti-flag (Abcam #ab125243) (for PA.FF) or mouse monoclonal anti-myc (Millipore #05-724) (for Myc.PA) antibodies.

Immunofluorescence assay

HeLa cells were grown on coverslips in 12-well plates and transfected with the plasmid DNA as described. About 44 to 48 h after transfection, the cells were washed with PBS and fixed with 3% (w/v) paraformaldehyde. The cells were washed again with PBS and treated with 0.1% (v/v) NP-40 (in PBS) for 15 min. Then, the cells were blocked for 30 min with 1% (w/v) non-fat milk powder (in PBS) and exposed to primary antibodies (mouse monoclonal anti HA, Santa Cruz #sc-7392, and/or anti-PA polyclonal rabbit antisera) diluted at 1:500 to 1:1000 for 1 h. The cells were washed twice with PBS and blocked a second time with 1% (w/v) non-fat milk. Following this, the cells were treated with goat anti-mouse IgG-Alexa-488 (Abcam #ab150117) and/or goat anti-rabbit IgG-Alexa-568 (Abcam #ab175471) secondary antibodies diluted at 1:300 for 60 min. The cell nuclei were visualized with DAPI. The coverslips with the cells were turned upside down on 2–3 μ l mounting medium, and the labeled proteins were visualized with a conventional fluorescent microscope (Olympus BX50) or a laser confocal microscope (Carl Zeiss LSM 700).

RNA extraction, first-strand cDNA synthesis, and qPCR

For quantitative analysis of transcripts in the cells by qPCR, the total RNA extraction was performed with a commercial kit (Qiagen #74,104) following the manufacturers' instructions. The integrity of the RNA samples was checked with denaturing agarose gel containing formaldehyde. First-strand cDNA synthesis was carried out with a MMLV reverse transcriptase enzyme (Toyobo #TRT-101 or Biotechrabbit #BR040020) by using 0.25–0.5 μ g total RNA and oligo-dT primer (for ACTB and MTCH2) or the primers specific for viral RNAs given in Table 1 (for vRNA of WSN: Seg8/WSN-QF/ for cRNA + mRNA of WSN: Seg8/WSN-QR/ for vRNA of DkPen: Seg8/DkPen-QF/ for cRNA + mRNA of DkPen: Seg8/DkPen-QR). The cDNA synthesis protocols were designed according to the enzyme manufacturers' guidelines. The qPCR was performed with FastStart Universal SYBR Green Master Mix (Roche #4913850001) by using the gene specific primers given in Table 1 (ACTB: ACTB-QF and ACTB-QR/ MTCH2: MTCH2-For and MTCH2-QR/ WSN viral RNAs: Seg8/WSN-QF and Seg8/WSN-QR/ DkPen RNAs: Seg8/DkPen-QF and Seg8/DkPen-QR). The qPCR cycling conditions were as follows: initial denaturation at 95 °C for 10 min, 45 cycles of

denaturation for 5 s at 95 °C, annealing at 52–58 °C for 10 s, and elongation at 72 °C for 20 s followed by melting curve analysis. The relative quantity of target gene transcripts in comparison to ACTB reference gene were defined.

Minireplicon assay

The viral RNA polymerase activity in the cells transfected with the MTCH2 coding plasmid was investigated with an influenza A virus minireplicon assay [23, 24]. The HEK293 cells were grown in 24-well plates (1×10^5 cells/well) under standard culture conditions for 20–24 h. The cells grown in each well were transfected with a set of minireplicon plasmids (pHH21-vNS-luc, pCAGGS-PB2, pCAGGS-PB1, pCAGGS-PA, and pCAGGS-NP), increasing amounts of pCHA-MTCH2 (30 ng, 100 ng, or 200 ng), and pSEAP for normalization. The total DNA quantity for each well was adjusted to 300 ng with the pCHA plasmid. At 24 h and 48 h post-transfection, secreted alkaline phosphatase (SEAP) (for normalization) that is expressed under the control of host RNA polymerase II (Pol II) and reporter firefly luciferase activities were determined, respectively. SEAP and luciferase activities were detected using the commercial kits (Roche #31420 and Promega #E1501).

Docking analysis

The 3D models of MTCH2 Δ N, MTCH2 v3, MTCH2:253–282, viral nPA and nP:280–359 proteins were predicted on the I-TASSER online platform (<https://zhanggroup.org/I-TASSER/>) using the I-TASSER algorithm [28]. The 3D model of the MTCH2 v1 protein (<https://alphafold.ebi.ac.uk/entry/Q9Y6C9>) predicted by AlphaFold [29, 30] was taken as a reference model. Interaction patterns of predicted MTCH2:253–282 peptide with nP:280–359 were generated on the ClusPro server (<https://cluspro.bu.edu>) with the ClusPro algorithm [31]. The carboxy-terminal region of MTCH2 consisting of 82 amino acid residues, which interacts with nPA in yeast cells, was highlighted in protein-protein docking analysis. Since the influenza A virus RdRp enzyme has a heterotrimeric structure, the interactions of the PA protein with PB2 and PB1 were taken into account in the docking analysis. Based on the influenza A/duck/Fujian/01/2002(H5N1) virus polymerase structure [32] provided in the RCSB Protein Data Bank (www.rcsb.org/structure/6QPF), the interaction points of PA-PB1 and PA-PB2 proteins were determined with the PDBsum [33] algorithm (<http://www.ebi.ac.uk/thornton-srv/databases/pdbsum/>) and a masking file of nPA was obtained for docking analysis. Using the interaction parameters determined for MTCH2:253–282 and nP:280–359 peptides, the possible protein-protein docking models were predicted with

the ClusPro algorithm. The affinity of protein-protein complexes was determined by calculating the Gibbs free energy change (ΔG) and the equilibrium dissociation constant (K_D) values using the PRODIGY (PROtein binDing enerGY prediction) web server [34]. The visualization of the results was performed using PyMOL software. In terms of Cluster numbers, the two most likely interaction models were presented.

Results

Identification of the human MTCH2 protein as an interactor of the viral PA protein

The interaction of the influenza A virus PA protein with the cellular MTCH2 protein was detected with the Y2H assay. The viral PA gene was cloned in a pGBD-C1 plasmid fused with GAL4.BD in different sizes and different orientations, and the plasmids encoding the bait proteins were obtained. However, it was determined only that the hybrid protein resulting from the fusion of the amino-terminal part of PA consisting of 359 amino acid residues (nPA) and the yeast GAL4.BD domain (148 amino acid residues) (Fig. 1A) interact with MTCH2 in the yeast cells. The yeast colony grown on the selective SD plate (without trp/leu/his/ade) and harboring MTCH2 cDNA showed high relative β -galactosidase activity (Fig. 1B). Sanger sequencing and subsequent BLAST analysis revealed that one of the library plasmids selected with Y2H-screening carries the partial cDNA of the MTCH2 gene (Fig. 1C) which encodes the carboxy-terminal part of the MTCH2 consisting of 82 amino acid residues fused with yeast GAL4.AD (Fig. 1D).

Expression and subcellular localization of the HA-tagged MTCH2 protein in transiently transfected cells

It is estimated that there are at least seven transcript isoforms for the human MTCH2 gene encoding proteins, ranging in size from 155 to 303 amino acids (<https://www.uniprot.org/uniprotkb/Q9Y6C9/entry#sequences>). In order to transiently express the MTCH2 protein in the mammalian cells and the native host of the influenza A viruses and to investigate the interaction of this protein with the viral PA, a cDNA coding MTCH2 v.3 consisting of 155 amino acids (Fig. 1D) was cloned in the pCHA plasmid in-frame with the sequence of the HA-tag (YPYDVPDYA). The plasmid DNA coding the HA-tagged MTCH2 v.3 (H.MTCH2) protein was transfected into HEK293 cells, and the transient expression of the protein was determined by Western blotting (Fig. 2A). Although the genes under the control of the chicken β actin promoter mostly have a high expression

level, Western blot analysis showed a low H.MTCH2 protein expression in the transiently transfected HEK293 cells. The intracellular localization of the H.MTCH2 protein transiently expressed in HeLa cells was detected by immunofluorescence staining. Similar to the native MTCH2 proteins localizing on the outer membrane of the mitochondria, transiently expressed H.MTCH2 proteins showed subcellular distribution pattern such as mitochondrial proteins in the cell cytoplasm (Fig. 2B).

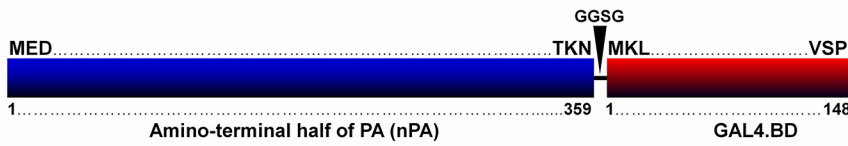
GST-pull down

The interaction between MTCH2 and PA protein in mammalian cells was evaluated in HEK293 cells co-expressing GST.MTCH2 and flag or myc-tagged PA (W) proteins. In case of possible interference, pull-down was carried out with both N-terminal myc-tagged PA and C-terminal flag-tagged PA proteins. Both the PA.FF (W) and Myc.PA (W) proteins co-precipitated with GST.MTCH2 protein, indicating an interaction between PA and MTCH2 proteins in mammalian cells (Fig. 3). This result suggests that PA protein interacts directly with MTCH2. However, due to the DSP crosslinking process prior to pull-down, an indirect interaction of these two proteins co-expressed in the cells cannot be excluded. There was a decrease in the electrophoretic mobility of myc/flag-tagged PA (Myc.PA / PA.FF) or GST-tagged PA proteins (GST-PA or PA-GST) subjected to pull-down compared to input (Figure S1). We believe that this is due to the interference of some components of the agarose beads with PA. Attempts with GST-tagged PA protein (GST.PA / H.MTCH2 or nPA.GST / H.MTCH2) did not yield any results (data not shown). It was thought that this may be related to the conformation of the fusion proteins and/or the protein expression levels. In particular, DkPen PA protein expression significantly inhibits the expression of the genes under the control of PolIII promoter [13], which makes co-precipitation experiments difficult. The expression of reporter green fluorescent protein (EGFP) is significantly inhibited in HEK293 cells co-transfected with plasmids encoding the DkPen PA proteins (Figure S2).

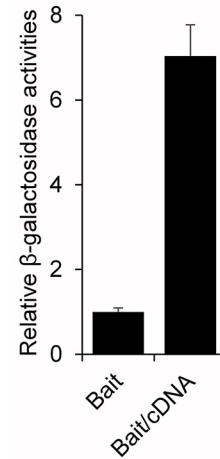
Influenza A virus replication in the MTCH2 gene knockdown cells

The effect of MTCH2 protein on the virus replication in mammalian cells were investigated in the HeLa cells. The MTCH2 gene in the cells was silenced with MTCH2-specific siRNA transfection. The efficiency of MTCH2 silencing was verified with qPCR. It was determined that the MTCH2 transcript level in the knockdown cells decreased by an average 96% compared to control cells (Fig. 4A). These cells were infected with human (WSN) and avian

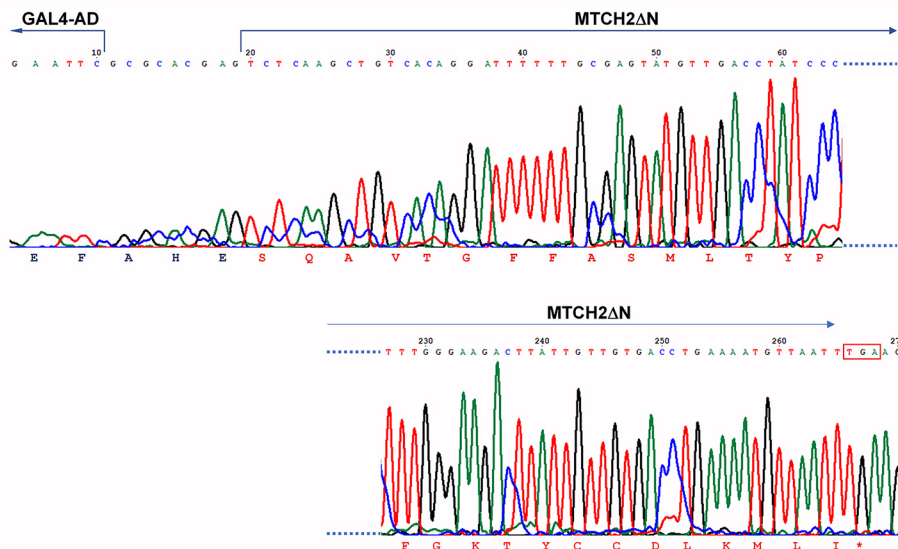
A



B



C



D

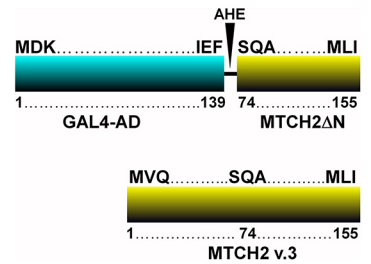
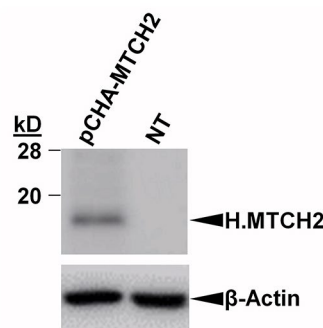


Fig. 1 Identification of influenza A virus PA interactor with Y2H assay. **A.** Schematic representation of the bait protein structure (nPA-GAL4.BD) used for Y2H screening. GGSG: A four-amino acid linker (Gly-Gly-Ser-Gly) added between viral nPA and GAL4.BD to give the protein a modular structure. **B.** Relative β -galactosidase activity of yeast cells harboring bait and candidate cDNA plasmids. GAL4.AD: yeast

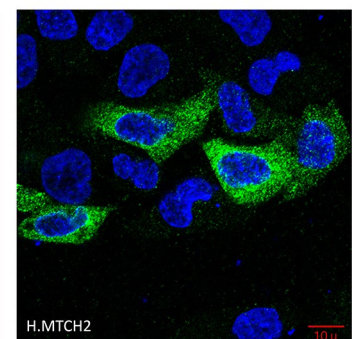
GAL4 transcription factor activation domain. GAL4.BD: Yeast GAL4 DNA binding domain. MTCHΔN: MTCH2 v.3 protein with 73 amino acid deletion at the amino terminal end. **C.** Sanger sequencing chromatogram of cDNA coding GAL4.AD-MTCH2ΔN. **D.** Schematic representation of structure of the candidate GAL4.AD-MTCH2ΔN and MTCH2 v3 proteins

Fig. 2 The expression and subcellular localization of H.MTCH2 proteins in the cells transfected with pCHA-MTCH2 plasmid. **A.** Western blot analysis of H.MTCH2 proteins expressed in HEK293 cells. The H.MTCH2 and β -Actin proteins were labeled with mouse monoclonal anti-HA and mouse monoclonal anti-actin antibodies, respectively. NT. Non-transfected cells. **B.** Subcellular localization of the H.MTCH2 in HeLa cells. The H.MTCH2 proteins were immunostained with mouse monoclonal anti-HA and goat anti-mouse IgG Alexa Fluor 488 conjugate antibodies and visualized via a laser confocal microscope (Carl Zeiss LSM 700)

A



B



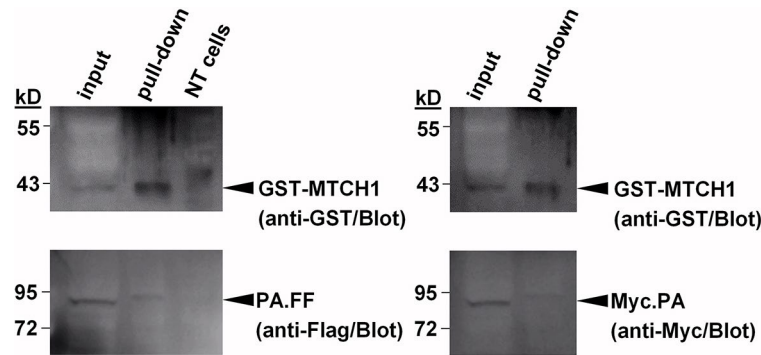


Fig. 3 Co-precipitation of the GST.MTCH2 and the viral PA proteins. The proteins were co-expressed in HEK293 cells with transfection of pCAGGS-GST-MTCH2/pCAGGS-PA.F or pCAGGS-GST-MTCH2/pCAGGS-Myc.PA plasmids. The GST.MTCH2 in the cell lysates were precipitated with glutathione-agarose beads and the proteins were analyzed with Western blotting. The proteins were separated using

SDS-PAGE, transferred to PVDF membrane, and blotted with rabbit polyclonal anti-GST (for GST.MTCH2), mouse monoclonal anti-flag (for PA.FF) and mouse monoclonal anti-myc (for Myc.PA) antibodies. They were then visualized using goat anti-rabbit or anti-mouse secondary antibodies conjugated to HRP and a chemiluminescence detection system

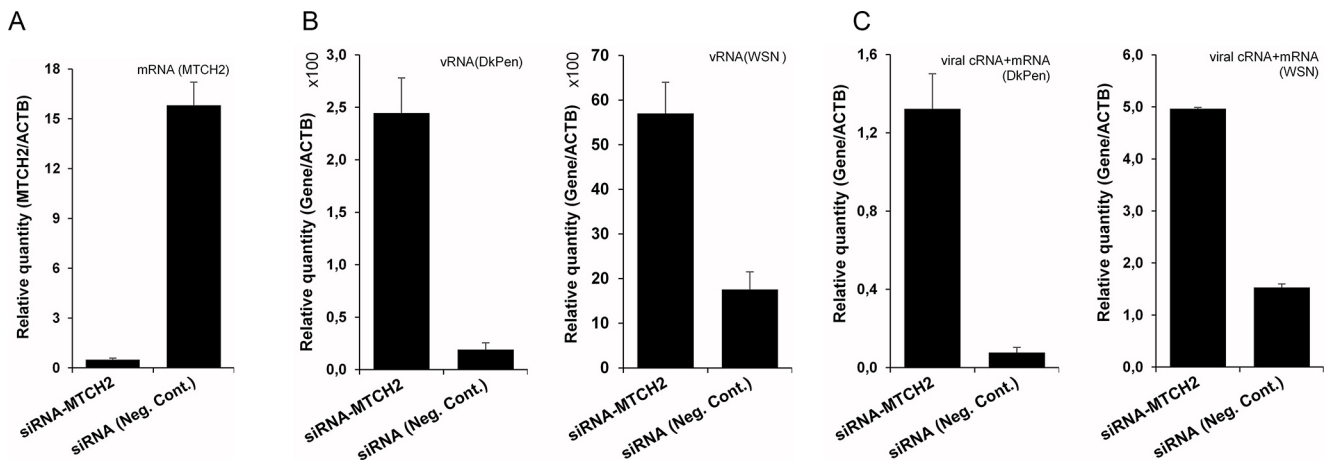


Fig. 4 Quantitative analysis of the viral and cellular RNAs in the HeLa cells transfected with siRNA and virus infected. (A) The MTCH2 gene transcript level in the cells transfected with MTCH2 gene specific siRNA. (B) The viral RNA quantities at eighth hour after infection

in the MTCH2 gene knockdown cells. (C) The viral cRNA+mRNA quantities at eighth hour after infection in the MTCH2 gene knockdown cells. The expression of the genes was normalized with the ACTB housekeeping gene (Gene/ACTB)

type (DkPen) influenza A viruses. The quantities of the viral RNA (vRNA), viral complementary RNA+viral mRNA (cRNA+mRNA) and cellular ACTB mRNA were determined in the total RNA isolated from the cells in the early stages of infection (8 h post infection) with qPCR. The viral RNA quantities were normalized with the ACTB transcript level and compared with the control cells transfected with negative control siRNA. In MTCH2 gene knockdown cells, the vRNA quantity of DKPen type viruses increased by an average of 92% in the early stage of infection, while the vRNA of WSN type viruses increased by 69% compared to the control cells (Fig. 4B). Similarly, an increase in the viral complementary RNAs was also detected in the cells. An average 94% and 69% increase of DKPen and WSN type virus cRNA+mRNA quantities was observed, respectively (Fig. 4C). These results revealed that the MTCH2 protein is a cellular factor having a down-regulatory effect

on influenza A virus replication. The MTCH2 was found to be more effective on avian DkPen type viruses than that of WSN. At 12 h post-infection, the MTCH2 gene knockdown HeLa cells were harvested and analyzed for viral PA and endogenous β -Actin proteins with western blotting (Fig. 5). In correlation with the viral RNA quantities given in Fig. 4, a significant increase in the amount of the viral protein was detected in the knockdown cells.

Effect of the MTCH2 protein on influenza A virus RdRp enzyme

Since the viral PA protein is a component of the influenza virus RNA polymerase, the effect of the MTCH2 protein on the viral RdRp enzyme was investigated with the mini-replicon assay [24]. The HEK293 cells grown in 24-well plates were co-transfected with minireplicon plasmids and

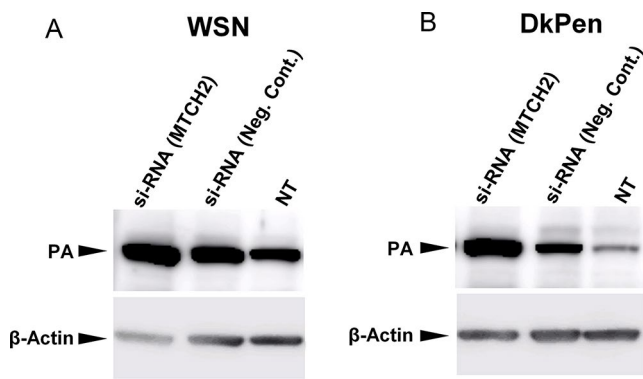


Fig. 5 Western blot analysis of the viral and cellular proteins in the siRNA transfected/virus-infected HeLa cells. The HeLa cells were infected with influenza A/WSN (A) or DkPen viruses (B). The proteins were separated on 10% polyacrylamide gel and transferred to PVDF membrane. Viral PA and cellular β -Actin proteins were labeled with polyclonal rabbit anti-PA and monoclonal mouse anti-actin antibodies, respectively. HRP-conjugated goat anti-rabbit IgG or anti-mouse IgG antibodies were used as secondary antibodies. The proteins were visualized with ECL detection kit. NT. Non-transfected cells

pCHA-MTCH2. Reporter luciferase activity in the cells was normalized with SEAP activity. The results showed that the increase of MTCH2 in transiently transfected HEK293 cells had a negative effect on both influenza A/WSN and DkPen virus RdRp (Fig. 6).

Intracellular localizations of co-expressed viral PA and H.MTCH2 proteins

Intracellular localization profiles of viral PA and MTCH2 proteins co-expressed in transiently transfected HeLa cells were examined by immunostaining. The viral PA protein shows nuclear and nucleocytoplasmic localization depending on its expression level (Fig. 7A). The MTCH2 protein, which is expressed alone in cells, gives a typical organelle protein location pattern in the cytoplasm (Figs. 2B and 7B). This result revealed that the co-expressed H.MTCH2 and viral PA proteins gave similar localization patterns and had a tendency to co-localization into the cells (Fig. 7C).

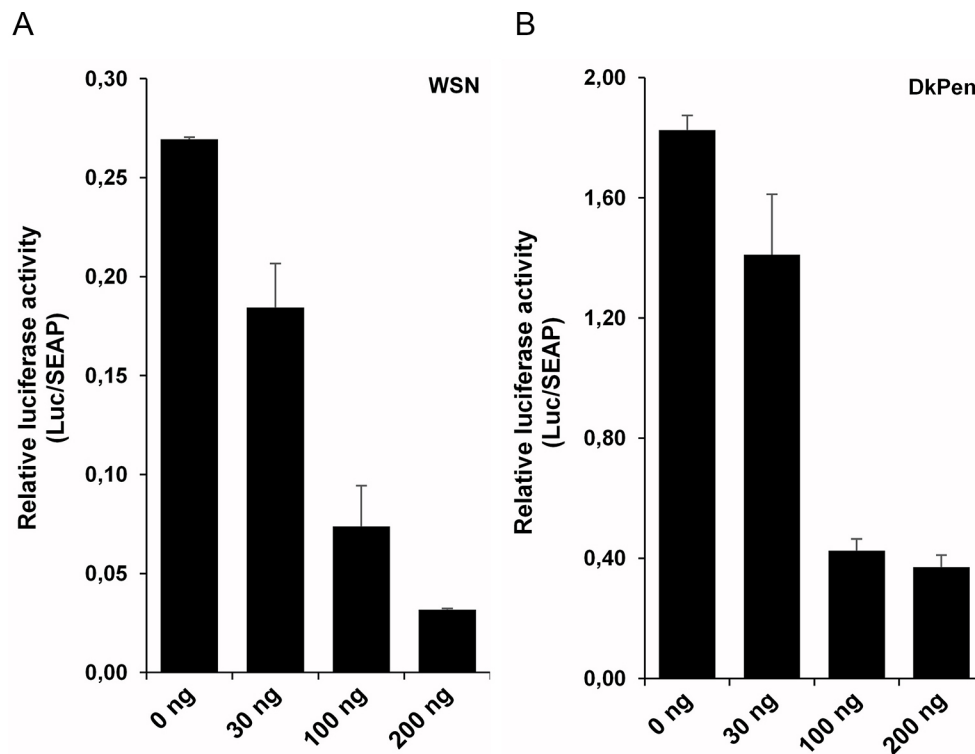


Fig. 6 The influenza A virus RdRp activities in HEK293 cells transfected with increasing amounts of pCHA-MTCH2 plasmid DNA encoding MTCH2 v3 protein. The viral RdRp activities were determined using the virus minireplicon assay. The HEK293 cells were co-transfected with plasmids encoding the RdRp subunits and NP protein of influenza A/WSN (A) or DkPen viruses (B). The cells grown in 24-well plate were co-transfected with constant amount of minirep-

licon plasmids (ng/well: 20 ng/pHH21-vNS-luc; 3 ng/pCAGGS-PB1/WSN or 10 ng/pCAGGS-PB1/DkPen; 3 ng/pCAGGS-PB2/WSN or 10 ng/pCAGGS-PB2/DkPen; 3 ng/pCAGGS-PA/WSN or 3 ng/pCAGGS-PA/DkPen; 30 ng/pCAGGS-NP/WSN or 30 ng/pCAGGS-NP/DkPen; 20 ng/pSEAP) and the pCHA-MTCH2 DNA in amounts shown in the figure. The reporter firefly luciferase activities were normalized with SEAP

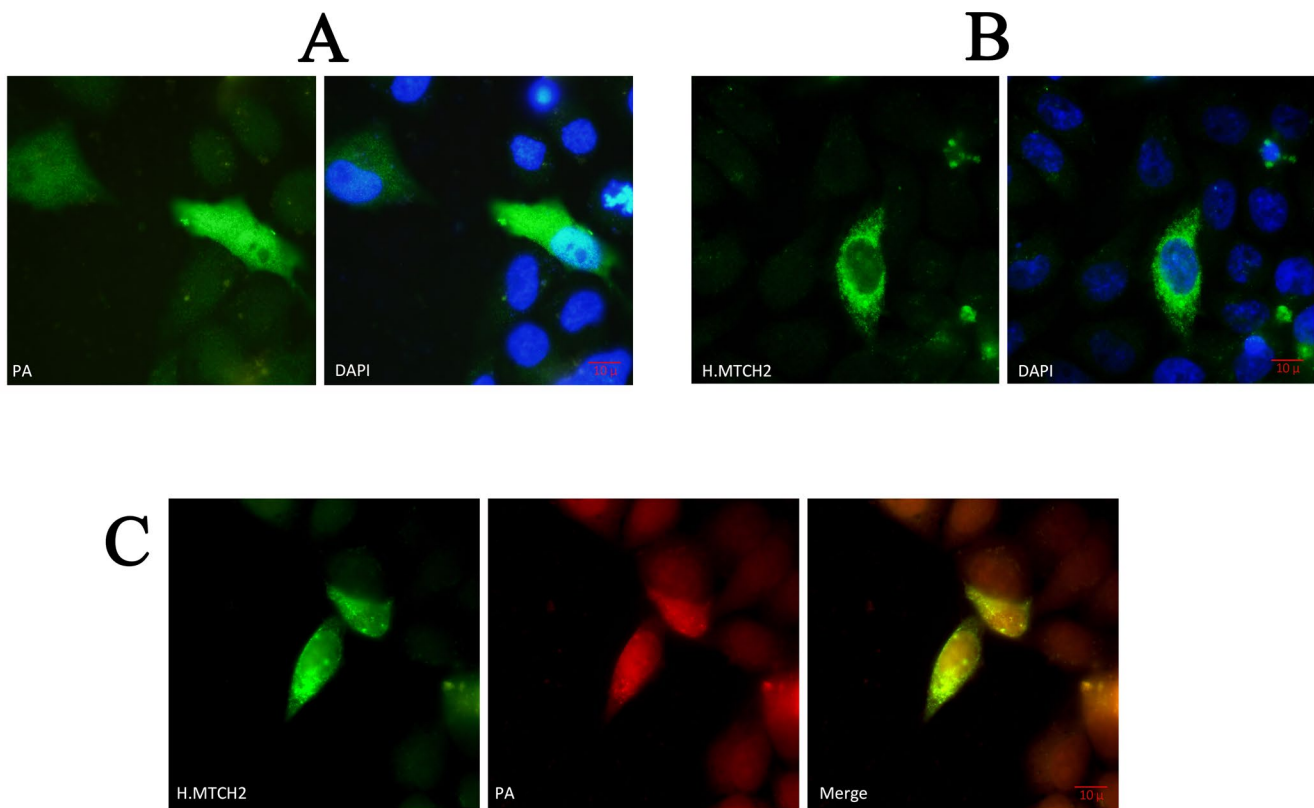


Fig. 7 The subcellular localization of transiently expressed viral PA and human H.MTCH2 proteins in the HeLa cells. The cells grown in 12-well plate were transfected with 0.5 μg of pCAGGS-PA and/or pCHA-MTCH2 plasmids and the proteins were immuno-stained at 48 h after transfection. The cells were analyzed with a conventional

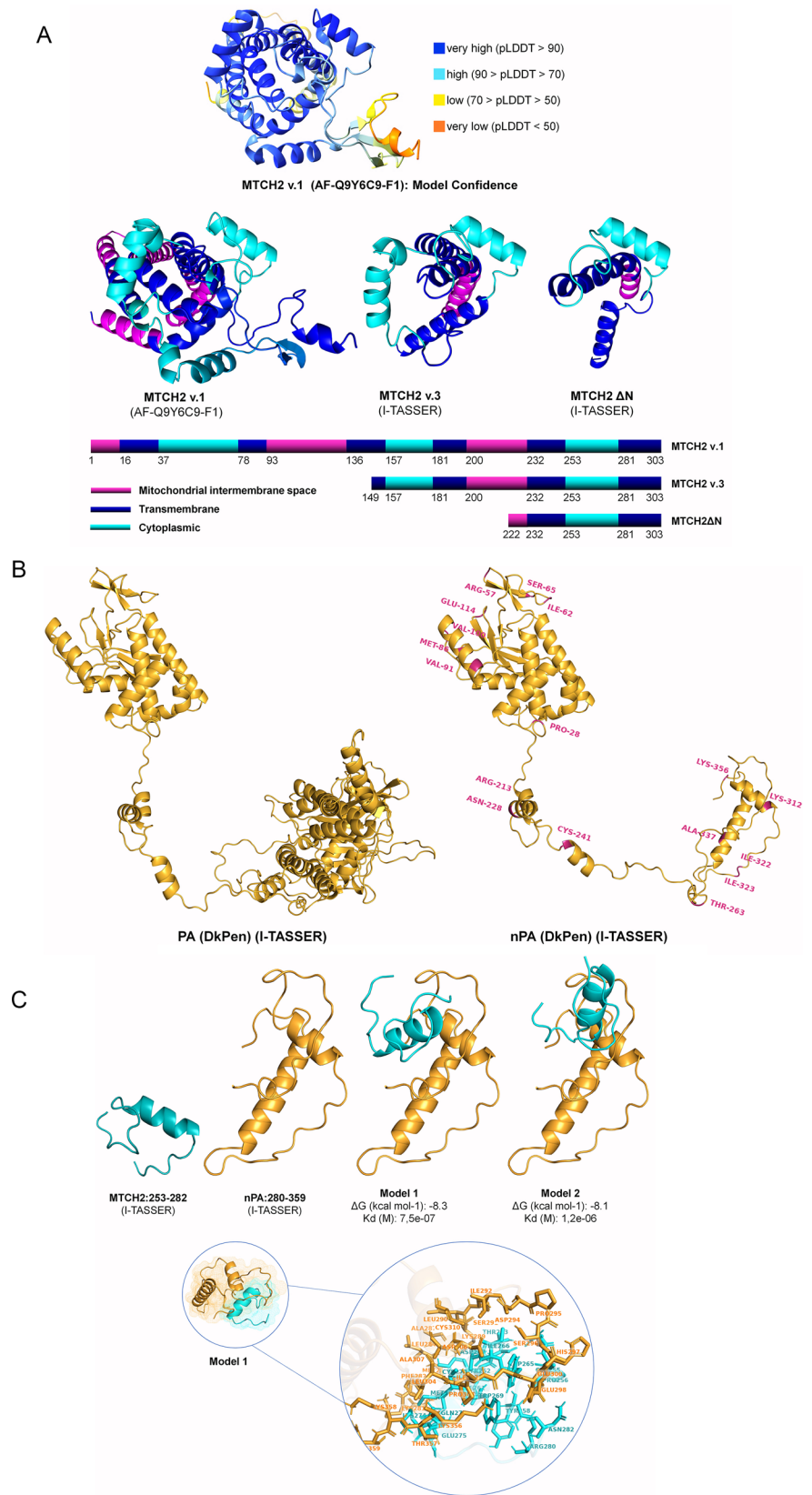
fluorescent microscope equipped with a peltier camera (Olympus DP72). **A.** The viral PA protein was expressed alone in the cells. **B.** The H.MTCH2 protein was expressed alone in the cells. **C.** The PA and H.MTCH2 proteins were co-expressed in the cells. Cell nuclei were stained with DAPI.

In silico prediction and interaction of MTCH2 and PA proteins

The MTCH2 protein is a multi-pass membrane protein located on the outer membrane of the mitochondria [35]. Using the predicted data of the MTCH2 protein in the UniProt protein data bank, the possible functional domains of the AlphaFold MTCH2 model (Q9Y6C9) and the I-TASSER models of MTCH2 v3, MTCH2:253–282, viral nPA and nPA:280–359 were visualized with PyMol software (Fig. 8). Three cytoplasmic domains were predicted for the MTCH2 v1. The MTCH2 ΔN peptide, interacting with the viral nPA protein in yeast cells, consists of 82 amino acid residues at the carboxy terminus of MTCH2 and carries a single cytoplasmic domain as alpha helix structure that is likely to interact with PA under native conditions (Fig. 8A). The 3D model of the influenza A/DkPen virus PA previously identified as the RdRp complex [32] and the nPA model predicted by the I-TASSER algorithm are given in Fig. 8B. The interaction of the viral PA protein with the MTCH2 was evaluated with ClusPro, ignoring the carboxy-terminal moiety and the regions involving in complex formation with PB2 and PB1.

As a result of protein-protein docking analysis between viral nPA and the third cytoplasmic domain of MTCH2 (MTCH2:253–282), it was found that the MTCH2:253–282 peptide formed clusters on the region of viral nPA covering the 280–350th amino acid residues in most of the predicted models (data not shown). Therefore, the predicted models of nPA:280–359 and MTCH2:253–282 peptides were subjected to protein docking analysis. The protein complex formation affinities of sixty models generated by ClusPro were determined using PRODIGY. Considering the ΔG and K_D values, two models with the highest rank were given in Fig. 8C. Interacting amino acid residues were detected in Model-1 having the highest binding affinity with values of “ ΔG : -8.4” and “ K_D :7.50E-07” (Fig. 8C, lower panel). In this model, 28 amino acid residues of nPA:280–359, which consists of 80 amino acids, are in close proximity to form a bond with the MTCH2:253–282 peptide. Considering the complex structure of the viral RdRp enzyme, it is thought that the Model-1 of the predicted models will have a higher probability of interaction with MTCH2.

Fig. 8 In silico prediction of the viral NP and human MTCH2 protein structures and protein-protein docking. **A.** The predicted 3D models of MTCH2 v.1 (AlfaFold) (AF-Q9Y6C9-F1-model_v4), MTCH2 v3 (I-TASSER) and MTCH2 Δ N (I-TASSER) proteins and possible domains of the protein in positioning on the mitochondrial membrane. **B.** The predicted 3D models of influenza A virus DkPen PA and carboxyterminal deleted PA (nPA) proteins generated with I-TASSER algorithm. **C.** Interaction models of MTCH2:253–282 and nP:280–359 with the highest rank of complex formation, and prominent interaction regions in Model 1. The 17 amino acid residues on the nPA (DkPen) protein that differ from the WSN PA are marked on the figure. These differences are P28L, R57Q, I62V, S65L, M86I, V91I, V100A, E114K, R213K, N228K, C241Y, T263S, K312R, I322V, I323V, A337S, and K356R



Discussion

In this paper, we described that the amino terminal half of the influenza virus PA (nPA) protein used as bait in the Y2H assay interacts with the MTCH2 protein, which has a similarity to mitochondrial carrier (MC) protein family members [2, 36]. The sequencing results of the cDNA encoding the candidate host protein identified with Y2H assay revealed that the peptide interacting with the nPA consists of an average of 82 amino acid residues from the carboxy terminal of MTCH2. Protein-protein docking analysis, which takes into account the localization pattern of the MTCH2 protein in the mitochondrial outer membrane, strengthened the idea that the region interacting with viral PA might be cytoplasmic alpha helix structure comprising amino acid residues 253 to 282.

It has been suggested that the human MTCH2 protein, located on the outer membrane of mitochondria, plays a critical role in embryonic development and is associated with apoptosis, which is programmed cell death [4, 5]. Although the biochemical function of MTCH2 in these events is not fully understood, it is obvious that it plays an important role in apoptosis process and mitochondria metabolic events. The apoptosis pathway, which is a natural process under certain conditions for multicellular organisms, is a situation that also affects the replication fate of viruses in many viral infections.

The results of many studies aimed at elucidating the cell–virus interaction clearly reveal that influenza A viruses interact with many cellular proteins during the replication process that take place from the attachment of the virus to the host cell to the release of progeny virus particles. While some of these proteins interacting with the virus have a negative effect on viral replication [37], some proteins facilitate the proliferation of the virus [38, 39]. It is of great importance to determine what these host proteins are, in which direction, and by what mechanisms they affect the viral replication in order to develop a new strategy to cope with viral infections. In this context, our studies conducted with a Y2H assay and mammalian cells showed that the influenza A virus PA protein interacts with the human MTCH2 protein (Figs. 1, 3 and 7). Significant increases in the viral RNAs and viral protein levels were detected in knockdown HeLa cells with MTCH2 gene-specific siRNAs (Figs. 4 and 5). Moreover, the influenza A DkPen type virus was found to replicate much more efficiently in MTCH2 gene knockdown cells than in the WSN type. The amino acid substitutions in DkPen and WSN PA proteins may also contribute to this difference. There is a total of 31 amino acid substitution in the DkPen and WSN PA proteins encoded via plasmid vectors. Of these, 17 amino acid substitutions were marked on nPA (Fig. 8B). It was concluded that this difference on

nPA was responsible for the negative effect especially on the expression of genes under the control of PolIII promoter.

Many avian-type influenza A viruses encounter host resistance in replication in mammalian cells and undergo a longer adaptation period [40]. It is known that the interaction of viral RNA polymerase subunits with some cellular protein factors also plays a role in this resistance arising [41, 42]. In contrast to MTCH2 gene knock-down cells, inhibition of the viral RdRp enzyme activity was observed in the cells with increased MTCH2 protein by transient transfection (Fig. 6). This may be a result of the negative effect of MTCH2 on the formation of the RdRp complex consisting of three subunits. However, since the virus replication is carried out by viral RdRp in the nucleus, it is not sufficient to explain the stimulation of viral replication in MTCH2-knock down cells only by the direct interaction of MTCH2 and the PA subunit. Therefore, due to its role in the apoptosis pathway, the MTCH2 protein may act as a mediator for the influenza virus to modulate apoptosis during the viral infection process.

The channeling of host cells into apoptosis during influenza A virus infection is thought to be a defense mechanism to inhibit viral replication. Almost all of the proteins encoded by influenza A viruses have a stimulating effect on the apoptosis pathway in host cells [12]. These proteins include the viral RdRp enzyme subunits as well as PB1-F2 and PA-X peptides synthesized by alternative processing of the genes encoding the subunits [43, 44]. In some studies, it has been suggested that the non-structural NS1 protein has a negative effect on apoptosis [43]. Therefore, it is suggested that influenza A viruses inhibit apoptosis in the early stages of infection to promote viral replication and activate apoptosis in later stages to accelerate the death of infected cells [45–47]. The upregulation of influenza A virus replication in MTCH2 gene knockdown cells may be due to two reasons. The MTCH2 protein can bind to the PA protein (or bind the PA to itself) and interfere with PA function or influence the apoptosis pathways to down-regulate virus replication under infection conditions.

In conclusion, it was discovered that the MTCH2 protein, which was found to interact with the influenza A virus PA by Y2H and GST pull-down assays, had a negative regulation effect on influenza A virus replication in mammalian cells. Although an indirect interaction cannot be completely ruled out, it was concluded that this effect was due to a direct interaction between the two proteins.

Supplementary Information The online version contains supplementary material available at <https://doi.org/10.1007/s11033-024-09584-5>.

Author contributions P.U., E.Ç., E.R. and K.T. conducted the experiments. P.U., E.Ç. and K.T. drafted the manuscript. K.N. and K.T. contributed to the conception and design of the study. All authors read and approved the final manuscript.

Funding This work was supported by a grant from the Scientific and Technological Research Council of Turkey (TÜBİTAK; grant no: SBAG-112S518).

Data availability The datasets used during the present study are available from the corresponding author upon reasonable request.

Declarations

Ethical approval In this study, neither human subjects nor animals were used.

Conflict of interest The authors declare that they have no known competing financial interests or personal relationships that could have appeared to influence the work reported in this paper.

References

- Guna A, Stevens TA, Inglis AJ et al (2022) MTCH2 is a mitochondrial outer membrane protein insertase. *Science* 378(6617):317–322. <https://doi.org/10.1126/science.add1856>
- Palmieri F (2008) Diseases caused by defects of mitochondrial carriers: a review. *Biochim Biophys Acta* 1777(7–8):564–578. <https://doi.org/10.1016/j.bbabo.2008.03.008>
- Palmieri F (2013) Mitochondrial metabolite carrier protein family. In: Lane MD, Lennarz WJ (eds) *Encyclopedia of Biological Chemistry*, 2nd edn. Academic, Waltham, pp 149–159
- Schwarz M, Andrade-Navarro MA, Gross A (2007) Mitochondrial carriers and pores: key regulators of the mitochondrial apoptotic program? *Apoptosis* 12(5):869–876. <https://doi.org/10.1007/s10495-007-0748-2>
- Zaltsman Y, Shachnai L, Yivgi-Ohana N et al (2010) MTCH2/MIMP is a major facilitator of tBID recruitment to mitochondria. *Nat Cell Biol* 12(6):553–562. <https://doi.org/10.1038/ncb2057>
- Maryanovich M, Zaltsman Y, Ruggiero A et al (2015) An MTCH2 pathway repressing mitochondria metabolism regulates haematopoietic stem cell fate. *Nat Commun* 6:7901. <https://doi.org/10.1038/ncomms8901>
- Rottiers V, Francisco A, Platov M et al (2017) MTCH2 is a conserved regulator of lipid homeostasis. *Obes (Silver Spring)* 25(3):616–625. <https://doi.org/10.1002/oby.21751>
- Ruggiero A, Aloni E, Korkotian E et al (2017) Loss of forebrain MTCH2 decreases mitochondria motility and calcium handling and impairs hippocampal-dependent cognitive functions. *Sci Rep* 7:44401. <https://doi.org/10.1038/srep44401>
- Rozenblatt-Rosen O, Deo RC, Padi M et al (2012) Interpreting cancer genomes using systematic host network perturbations by tumour virus proteins. *Nature* 487(7408):491–495. <https://doi.org/10.1038/nature11288>
- Nainu F, Shiratsuchi A, Nakanishi Y (2017) Induction of apoptosis and subsequent phagocytosis of Virus-infected cells as an antiviral mechanism. *Front Immunol* 8:1220. <https://doi.org/10.3389/fimmu.2017.01220>
- Rex DAB, Keshava Prasad TS, Kandasamy RK (2022) Revisiting regulated cell death responses in viral infections. *Int J Mol Sci* 23(13). <https://doi.org/10.3390/ijms23137023>
- Ampomah PB, Lim LHK (2020) Influenza a virus-induced apoptosis and virus propagation. *Apoptosis* 25(1–2):1–11. <https://doi.org/10.1007/s10495-019-01575-3>
- CaGlavan E, Turan K (2021) Expression profiles of interferon-related genes in cells infected with influenza A viruses or transiently transfected with plasmids encoding viral RNA polymerase. *Turk J Biol* 45(1):88–103. <https://doi.org/10.3906/biy-2005-73>
- Nayak DP, Hui EK, Barman S (2004) Assembly and budding of influenza virus. *Virus Res* 106(2):147–165. <https://doi.org/10.1016/j.virusres.2004.08.012>
- Plotch SJ, Bouloy M, Krug RM (1979) Transfer of 5'-terminal cap of globin mRNA to influenza viral complementary RNA during transcription in vitro. *Proc Natl Acad Sci U S A* 76(4):1618–1622. <https://doi.org/10.1073/pnas.76.4.1618>
- Krug RM, Morgan MA, Shatkin AJ (1976) Influenza viral mRNA contains internal N6-methyladenosine and 5'-terminal 7-methylguanosine in cap structures. *J Virol* 20(1):45–53. <https://doi.org/10.1128/JVI.20.1.45-53.1976>
- Plotch SJ, Tomasz J, Krug RM (1978) Absence of detectable capping and methylating enzymes in influenza virions. *J Virol* 28(1):75–83. <https://doi.org/10.1128/JVI.28.1.75-83.1978>
- Shirayama R, Shoji M, Sriwilaijaroen N, Hiramatsu H, Suzuki Y, Kuzuhara T (2016) Inhibition of PA endonuclease activity of influenza virus RNA polymerase by Kampo medicines. *Drug Discov Ther* 10(2):109–113. <https://doi.org/10.5582/ddt.2016.01010>
- Kim JH, Hatta M, Watanabe S, Neumann G, Watanabe T, Kawakita Y (2010) Role of host-specific amino acids in the pathogenicity of avian H5N1 influenza viruses in mice. *J Gen Virol* 91(Pt 5):1284–1289. <https://doi.org/10.1099/vir.0.018143-0>
- Sakabe S, Takano R, Nagamura-Inoue T et al (2013) Differences in cytokine production in human macrophages and in virulence in mice are attributable to the acidic polymerase protein of highly pathogenic influenza A virus subtype H5N1. *J Infect Dis* 207(2):262–271. <https://doi.org/10.1093/infdis/jis523>
- James P, Halladay J, Craig EA (1996) Genomic libraries and a host strain designed for highly efficient two-hybrid selection in yeast. *Genetics* 144(4):1425–1436. <https://doi.org/10.1093/genetics/144.4.1425>
- Nagata K, Saito S, Okuwaki M et al (1998) Cellular localization and expression of template-activating factor I in different cell types. *Exp Cell Res* 240(2):274–281. <https://doi.org/10.1006/excr.1997.3930>
- Pham PTV, Turan K, Nagata K, Kawaguchi A (2018) Biochemical characterization of avian influenza viral polymerase containing PA or PB2 subunit from human influenza A virus. *Microbes Infect* 20(6):353–359. <https://doi.org/10.1016/j.micinf.2018.04.003>
- Turan K, Mibayashi M, Sugiyama K, Saito S, Numajiri A, Nagata K (2004) Nuclear MxA proteins form a complex with influenza virus NP and inhibit the transcription of the engineered influenza virus genome. *Nucleic Acids Res* 32(2):643–652. <https://doi.org/10.1093/nar/gkh192>
- Sugiyama K, Kawaguchi A, Okuwaki M, Nagata K (2015) pp32 and APRIL are host cell-derived regulators of influenza virus RNA synthesis from cRNA. *Elife* 4. <https://doi.org/10.7554/eLife.08939>
- Sambrook J, Fritsch ER, Maniatis T (1989) *Molecular cloning: a Laboratory Manual*. Cold Spring Harbor Laboratory Press, In, Cold Spring Harbor, NY
- Gietz RD, Schiestl RH (2007) Large-scale high-efficiency yeast transformation using the LiAc/SS carrier DNA/PEG method. *Nat Protoc* 2(1):38–41. <https://doi.org/10.1038/nprot.2007.15>
- Zhang Y (2008) I-TASSER server for protein 3D structure prediction. *BMC Bioinformatics* 9:40. <https://doi.org/10.1186/1471-2105-9-40>
- Jumper J, Evans R, Pritzel A et al (2021) Highly accurate protein structure prediction with AlphaFold. *Nature* 596(7873):583–589. <https://doi.org/10.1038/s41586-021-03819-2>
- Varadi M, Anyango S, Deshpande M et al (2022) AlphaFold protein structure database: massively expanding the structural coverage of protein-sequence space with high-accuracy models. *Nucleic Acids Res* 50(D1):D439–D444. <https://doi.org/10.1093/nar/gkab1061>

31. Kozakov D, Hall DR, Xia B et al (2017) The ClusPro web server for protein-protein docking. *Nat Protoc* 12(2):255–278. <https://doi.org/10.1038/nprot.2016.169>
32. Fan H, Walker AP, Carrique L et al (2019) Structures of influenza A virus RNA polymerase offer insight into viral genome replication. *Nature* 573(7773):287–290. <https://doi.org/10.1038/s41586-019-1530-7>
33. Laskowski RA (2007) Enhancing the functional annotation of PDB structures in PDBsum using key figures extracted from the literature. *Bioinformatics* 23(14):1824–1827. <https://doi.org/10.1093/bioinformatics/btm085>
34. Xue LC, Rodrigues JP, Kastriitis PL et al (2016) PRODIGY: a web server for predicting the binding affinity of protein-protein complexes. *Bioinformatics* 32(23):3676–3678. <https://doi.org/10.1093/bioinformatics/btw514>
35. Gross A (2005) Mitochondrial carrier homolog 2: a clue to cracking the BCL-2 family riddle? *J Bioenerg Biomembr* 37(3):113–119. <https://doi.org/10.1007/s10863-005-6222-3>
36. Ruprecht JJ, Kunji ERS (2020) The SLC25 mitochondrial carrier family: structure and mechanism. *Trends Biochem Sci* 45(3):244–258. <https://doi.org/10.1016/j.tibs.2019.11.001>
37. Kodym R, Kodym E, Story MD (2009) 2'-5'-Oligoadenylate synthetase is activated by a specific RNA sequence motif. *Biochem Biophys Res Commun* 388(2):317–322. <https://doi.org/10.1016/j.bbrc.2009.07.167>
38. Chen G, Liu CH, Zhou L, Krug RM (2014) Cellular DDX21 RNA helicase inhibits influenza A virus replication but is counteracted by the viral NS1 protein. *Cell Host Microbe* 15(4):484–493. <https://doi.org/10.1016/j.chom.2014.03.002>
39. Kocmar T, Caglayan E, Rayaman E, Nagata K, Turan K (2022) Human sorting nexin 2 protein interacts with Influenza A virus PA protein and has a negative regulatory effect on the virus replication. *Mol Biol Rep* 49(1):497–510. <https://doi.org/10.1007/s11033-021-06906-9>
40. McKellar J, Rebendenne A, Wencker M, Moncorge O, Goujon C (2021) Mammalian and avian host cell influenza A restriction factors. *Viruses* 13(3). <https://doi.org/10.3390/v13030522>
41. Almond JW (1977) A single gene determines the host range of influenza virus. *Nature* 270(5638):617–618. <https://doi.org/10.1038/270617a0>
42. Subbarao EK, London W, Murphy BR (1993) A single amino acid in the PB2 gene of influenza A virus is a determinant of host range. *J Virol* 67(4):1761–1764. <https://doi.org/10.1128/JVI.67.4.1761-1764.1993>
43. Gao H, Sun H, Hu J et al (2015) Twenty amino acids at the C-terminus of PA-X are associated with increased influenza A virus replication and pathogenicity. *J Gen Virol* 96(8):2036–2049. <https://doi.org/10.1099/vir.0.000143>
44. Gui R, Chen Q (2021) Molecular events involved in Influenza A Virus-Induced cell death. *Front Microbiol* 12:797789. <https://doi.org/10.3389/fmicb.2021.797789>
45. Chen W, Calvo PA, Malide D et al (2001) A novel influenza A virus mitochondrial protein that induces cell death. *Nat Med* 7(12):1306–1312. <https://doi.org/10.1038/nm1201-1306>
46. Ehrhardt C, Wolff T, Pleschka S et al (2007) Influenza A virus NS1 protein activates the PI3K/Akt pathway to mediate antiapoptotic signaling responses. *J Virol* 81(7):3058–3067. <https://doi.org/10.1128/JVI.02082-06>
47. Zhirnov OP, Konakova TE, Wolff T, Klenk HD (2002) NS1 protein of influenza A virus down-regulates apoptosis. *J Virol* 76(4):1617–1625. <https://doi.org/10.1128/jvi.76.4.1617-1625.2002>

Publisher's Note Springer Nature remains neutral with regard to jurisdictional claims in published maps and institutional affiliations.

Springer Nature or its licensor (e.g. a society or other partner) holds exclusive rights to this article under a publishing agreement with the author(s) or other rightsholder(s); author self-archiving of the accepted manuscript version of this article is solely governed by the terms of such publishing agreement and applicable law.